



Numerical investigation of the contribution of the soil-structure interaction effects to the seismic performance and the losses of RC buildings

M.V. Requena-Garcia-Cruz^{a,*}, E. Romero-Sánchez^a, A. Morales-Esteban^{a,b}

^a Department of Building Structures and Geotechnical Engineering, University of Seville, Spain

^b Instituto Universitario de Ciencias de la Construcción, University of Seville, Spain

ARTICLE INFO

Keywords:

Seismic performance
Loss assessment
Reinforced concrete buildings
Soil-structure interaction (SSI)
3D finite elements
Direct method

ABSTRACT

Seismic vulnerability and loss analyses of buildings are usually estimated under the fixed-based condition, omitting the soil-structure interaction (SSI) effects. However, according to the literature and the seismic damage due to past events, mid-to high-rise buildings located on soft soils can present a worse seismic performance. This manuscript aims to investigate whether the SSI effects affect the seismic performance and the losses of reinforced concrete (RC) buildings. To do so, a real 5-storey RC building has been selected as the case study. It was built prior to restrictive Spanish seismic codes. The building was constructed over soft alluvial strata and it has a shallow foundation. The area is characterised by a moderate seismic hazard. Nonlinear static analysis (NLSA) and incremental dynamic analysis (IDA) have been performed to assess the seismic behaviour and the losses expected of the case study building. The calculations have been done in the OpenSees finite-element framework. The direct method has been used to model the SSI. The results have been obtained for the fixed-base and for the SSI models. The numerical outcomes have shown the remarkable effect of the SSI on the fragility and on the performance of these structures. It has been observed that the severe damage expected can be worsened by up to 38% if SSI is taken into account. Additionally, the soft-storey mechanism at the ground floor concentrates all the damage expected, showing that this is the most seismic vulnerable part of the building (owing to higher interstorey-drift ratios and peak floor acceleration values). The losses expected derived for structural and non-structural components have been 140% higher if the SSI is considered.

1. Introduction

The soil-structure interaction (SSI) effects have been traditionally considered to be beneficial in the seismic response of buildings (Anand and Satish Kumar, 2018). Hence, a major part of the seismic vulnerability analyses of buildings is usually done under the fixed-based (FB) condition, omitting the SSI. Nevertheless, according to the literature and to the seismic damage due to past events, mid-to high-rise buildings located on soft soils can present a worse seismic performance. This points out the detrimental effects of the SSI. In fact, as shown in (Requena-Garcia-Cruz et al., 2022a), in such cases, the maximum capacity of the models can be reduced by up to 15% if the SSI is considered. In (Asadi-Ghoozhi et al., 2022), lower values of the safety factor of foundations lead to a considerable decrease in the structural behaviour, meaning that a softer soil can produce a worse behaviour of the building.

The SSI effects can be taken into account by modifying the stiffness and the behaviour of the system at its base. Among all the possible

modelling approaches, the most common are the Beam on Nonlinear Winker method (BNWM) and the direct modelling of the soil. The BNWM allows bearing in mind the SSI by means of nonlinear springs. This method is usually implemented in seismic vulnerability analyses (Asadi-Ghoozhi et al., 2022; Rajeev and Tesfamariam, 2012; Kamal et al., 2022). This is a simple procedure, which requires the greatest effort on the calibration of the springs. In (Behnamfar and Banizadeh, 2016), dynamic analyses were performed by using 10 earthquake records for different reinforced concrete (RC) building and for different soil types. The SSI was modelled following the BNWM method, obtaining that the seismic vulnerability is increased on soft soils. In (Nguyen and Shin, 2021), an idealised RC structure was subjected to 20 ground motions, modelling the soil with springs and dashpots. The mass and the moment of inertia of the footing were lumped at the bottom of the columns. The results indicated that a higher shear wave velocity (V_s) of the soil leads to a higher ductility capacity. This means that the more rigid the soil is, the more deformation capacity the building has. Despite being widely used in seismic analyses, the BNWM method leads to

* Corresponding author.

E-mail addresses: mrequenal@us.es (M.V. Requena-Garcia-Cruz), eromero13@us.es (E. Romero-Sánchez), ame@us.es (A. Morales-Esteban).

<https://doi.org/10.1016/j.dibe.2022.100096>

Received 26 July 2022; Received in revised form 4 October 2022; Accepted 22 October 2022

Available online 26 October 2022

2666-1659/© 2022 The Authors. Published by Elsevier Ltd. This is an open access article under the CC BY-NC-ND license (<http://creativecommons.org/licenses/by-nc-nd/4.0/>).

| List of abbreviations | | Type of analyses | |
|-----------------------|--------------------------------------|------------------|--|
| <i>Parameters</i> | | NLSA | Nonlinear static analysis |
| V_s | Shear wave velocity | IDA | Incremental dynamic analysis |
| θ_{um} | Ultimate chord rotation | PBEE | Performance-based earthquake engineering |
| θ_y | Yielding chord rotation | PEER | Pacific Earthquake Engineering Research Centre |
| N_{spt} | Number of standard penetration tests | NRHA | Nonlinear time storey analysis |
| V_b | Basal shear | EDP | Engineering demand parameter |
| W_{tot} | Total weight of the building | IM | Intensity measure |
| d_{top} | Rooftop displacement | IDR | Interstorey drift ratio |
| H_{tot} | Total height of the building | PFA | Peak floor acceleration |
| S_a | Spectral acceleration | PSHA | Probabilistic seismic hazard analysis |
| <i>Miscellaneous</i> | | PGA | Peak ground acceleration |
| SSI | Soil-structure interaction | GM | Ground motion |
| FB | Fixed-based | CDR | Capacity/demand ratio |
| CS | Considering the SSI | LS | Limit state |
| BNWM | Beam on Nonlinear Winker method | DL | Damage limitation |
| RC | Reinforced concrete | SD | Severe damage |
| | | NC | Near collapse |

certain assumptions. Such is the case of the impossibility of considering deeper layers of soils rather than the superficial ones or the specific modelling of the foundation and its stiffness (modelled as concentrated at the base of RC frames).

Contrariwise, the direct method enables obtaining more realistic results since the complete SSI system (foundation and soil) is modelled as solid elements instead of springs. Furthermore, it is possible to model the complete geotechnical profile. However, the direct method is not usually followed in seismic vulnerability analyses due to its high computational cost and to the large number of input data required (Requena-Garcia-Cruz et al., 2022b). Nevertheless, in (Requena-Garcia-Cruz et al., 2022a), both modelling methods were numerically compared, concluding that the results obtained from nonlinear static analyses (NLSA) (peak strength and deformation) could vary by up to 15%. In this work, more conservative results were obtained for the models considering the direct method for different types of soil. In (Tomeo et al., 2017), both modelling approaches were compared for a two-dimensional RC frame designed according to the regulations. The soil classes suggested by the Eurocode-8 (EC8) were considered to define the mechanical properties of the soil beneath the building. The study showed that the SSI affects the seismic demand in terms of maximum base shear and maximum interstorey drift ratio with a significant difference depending on the modelling approach.

There is a lack of works considering the SSI and performing nonlinear dynamic analyses, such as incremental dynamic analyses (IDA). This is even greater if the SSI is modelled following the direct method. This is due to the higher computational cost that is required, despite allowing more exhaustive analyses. Furthermore, it is even more problematic to find studies on the loss assessment of RC buildings considering the SSI.

It is commonly known that minimising the consequences of eventual seismic events is the main goal of seismic risk analyses (Pinto and Franchin, 2014). Apart from seismic safety and vulnerability, additional indicators, such as social and economic, should also be borne in mind (Bommer et al., 2002). Indeed, aspects like the economic losses associated with repair/replacement actions, the disruption of the use of the buildings or the relocation of occupants can be useful to quantify the consequences of an earthquake (Cardone and Perrone, 2017). In this context, the so-called Performance-Based Earthquake Engineering (PBEE) approach, proposed by the Pacific Earthquake Engineering Research Centre (PEER), is the most common one implemented (Caruso et al., 2019). This approach quantifies the seismic performance and the losses following a probabilistic approach and considering different sources of uncertainty (Aslani and Miranda, 2005): the seismic hazard,

the structural performance and the seismic damage. In (Khosravikia et al., 2018), this procedure was followed to assess the losses stemming from the consideration of the SSI. This was modelled with the BNWM, for idealised RC structures. It was concluded that there is a 40% probability of increasing the losses of up to 10% compared to the fixed models if the structures are on moderately soft soils. In (Mitropoulou et al., 2016), a similar modelling procedure was used, concluding that the foundation system contributes considerably to the overall fragility performance of the buildings. Similar results were obtained in (Arboleda-Monsalve et al., 2020), which analysed high buildings. In this case, by considering SSI effects in the numerical analyses, the losses expected can be increased by up to 33%.

This manuscript aims to investigate if the SSI effects influence the seismic performance and the expected losses of RC buildings. To do so, a real 5-storey RC building, built prior to restrictive Spanish seismic codes, has been selected as the case study. The structure presents irregularities in the infills distributions, it is located over soft alluvial strata and it has a shallow foundation. The area is characterised by a moderate seismic hazard. The main contributions of this work are: i) the assessment of the seismic behaviour, the fragility and the expected losses (considering both structural and non-structural components) of the case study building; ii) these types of analyses have not been yet done for the area and the type of building; iii) both NLSA and IDA have been performed on 3D finite element models developed in OpenSees to realistically reproduce the entire system's behaviour (soil + foundation + structure), instead of the simple BNWM; and, iv) a method to assess and to compute the local damage, the fragility curves and the losses considering the SSI to fill in the gap identified in the analysis of the state of the art.

2. Method

This work is based on the PEER-PBEE approach to compute the fragility and the losses expected in RC buildings (Fig. 1). It is based on four main steps considering different levels of uncertainty that are later described: the seismic hazard, the structural performance, the seismic damage and the loss analysis. The models and the structural analyses have been performed in OpenSees (McKenna et al., 2000). This is a finite element software package specific for the structural and the seismic assessment of structures, being the one most implemented for this type of analyses (Requena-Garcia-Cruz et al., 2022a; Asadi-Ghoozdi et al., 2022; Rajeev and Tesfamariam, 2012; Kamal et al., 2022; Behnamfar and Banizadeh, 2016; Tomeo et al., 2017; Arboleda-Monsalve et al., 2020). The results have been pre- and post-processed in STKO (Petra

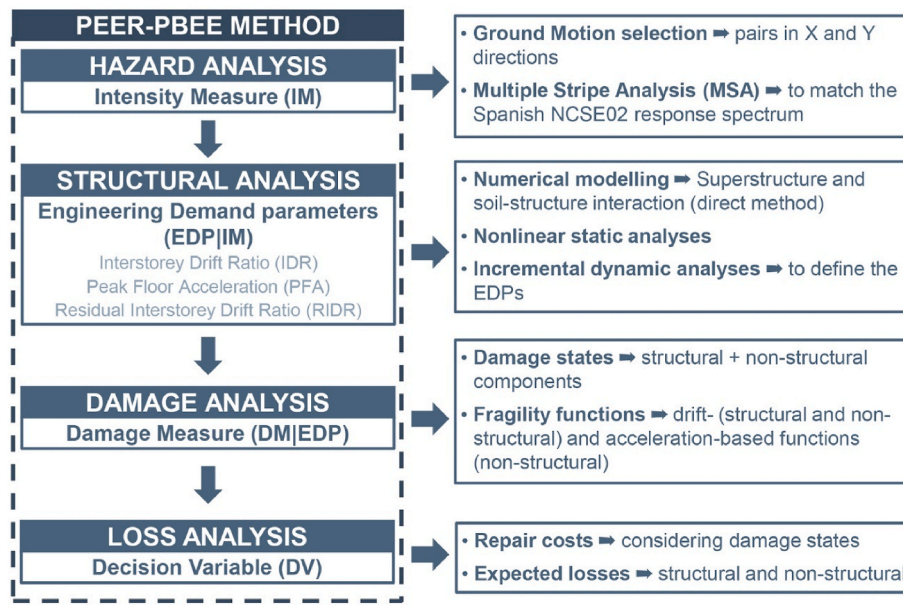


Fig. 1. Flowchart of this work based on the PEER-PBEE approach.

et al., 2017) and Matlab (The MathWorks Inc, 2018). The models analysed have been the fixed-base (FB) and the direct method for considering the soil (CS).

2.1. Structural and seismic hazard analyses

NLSA have been carried out to obtain the capacity of the models. To do so, a load- and a displacement-control integrator have been used to perform the gravitational and the NLSA steps, respectively. Previously, a modal analysis has been carried out to define the horizontal load pattern. All types of analyses have been performed in parallel in OpenSees given the size of the models.

The engineering demand parameters (EDPs) have been defined through nonlinear response-history analyses (NRHA) at different intensity measure (IM) levels. This type of analysis is commonly known as IDA. In this case, three EDPs have been computed for all models from the IDA: the interstorey drift ratio (IDR), the peak floor acceleration (PFA) and the residual interstorey drift ratio (RIDR).

The case study selected is located in Seville (Spain), for which the reference peak ground acceleration (PGA) is 0.09 g. This value is provided by the update of the probabilistic seismic hazard analysis (PSHA), recently carried out (Spanish Ministry of Public Works [Ministerio de Fomento de España], 2012). The PGA is expressed for a soil type A, rock. A set of real GMs (ground motion) records has been selected and they have been increased by means of a multiple stripe analysis (MSA), considering eight levels of IM, ranging from 0.0225 g to 0.54 g. The GMs have been selected to match Seville’s target spectrum based on the spectral acceleration (S_a) (Fig. 2), which is the seismic parameter most related to the seismic response of the structures, and according to the probabilistic method presented in (Morales-Esteban et al., 2012). The target spectrum has been defined in line with the Spanish seismic code NCSE02 (Spanish Ministry of Public Works [Ministerio de Fomento de España], 2002). Ten GMs have been found that match the response spectrum ranging from 0.85 to 1.15. Five GMs have been finally selected for the analyses as suggested in other similar works (Behnamfar and Banizadeh, 2016). They have been applied in the two orthogonal directions of the models (X and Y). The GMs applied to the FB model have been obtained from reading the results at the base of the model, after applying the GM for the soil type A at the bedrock.

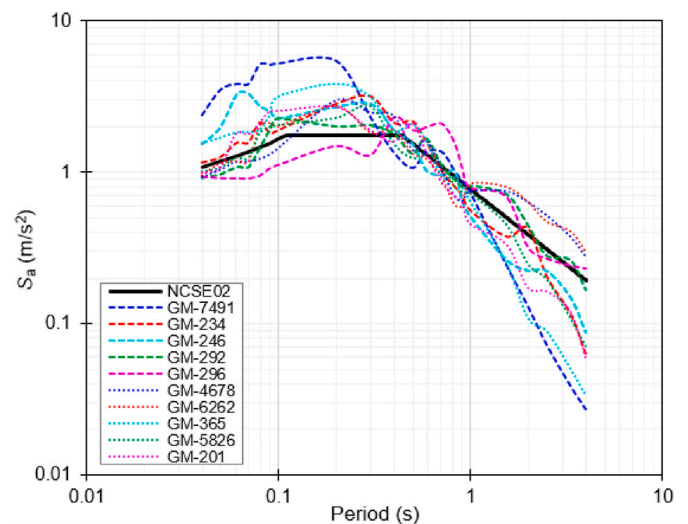


Fig. 2. Response spectrum for Seville and the GMs selected for the analyses.

2.2. Seismic safety and damage analysis

In the case of RC buildings, damage in the vertical components is considerably more usual than in the beams, as concluded in several works (Requena-Garcia-Cruz et al., 2021; Caruso, 2019). Hence, in this work, the damage in the structural components has only been considered for the columns.

First, the results of the NLSA and the N2-method (Fajfar and Gasperšič, 1996) have been considered to determine the seismic safety of the models. To do so, the capacity/demand ratio (CDR) established in the EC8 part 3 (EC8-3) (European Union and Eurocode-8, 2005) has been used. This is computed as the ratio between the limit state (LS) considered and the seismic demand (defined according to the N2-method). The ratio has been obtained for the significant damage (SD) LS. Additionally, the damage limitation (DL) and the near collapse (NC) LS have been computed. The NC is calculated considering the ultimate chord rotation (θ_{um}). The SD is determined as 3/4 of θ_{um} . The DL is worked out by means of the yielding chord rotation (θ_y). The formulae of each parameter are established in the EC8-3. Each damage state has

been calculated when the demand chord of one column reaches its capacity values.

For the fragility analysis, four LS have been considered to define the fragility functions following the procedure established in (Aslani and Miranda, 2005): DS1, light damage; DS2, moderate damage; DS3, severe damage; and, DS4, collapse. Drift-based fragility functions have been defined to estimate the damage in the structural components, i.e., considering the chord rotation. They have been defined according to the work developed for non-ductile RC frames presented in (Aslani and Miranda, 2005). In the case of the non-structural components, two types of fragility functions have been considered. Drift-based fragility functions have been adopted from the work developed by (Cardone and Perrone, 2015) for infill masonry walls. These functions were experimentally obtained for RC buildings built before the 70s, which share similar structural and constructive characteristics of the case study building. Damage to acceleration-sensitive non-structural components have been defined according to the well-known American procedure named HAZUS (National Institute of Building Sciences and Federal Emergency Management Agency (NIBS and FEMA), 2003).

2.3. Losses analysis

The total expected loss ($E[\text{Loss}_T | \text{IM}]$) as a function of the ground motion intensity (IM) has been calculated as the sum of three aspects: i) the losses resulting from the collapse of the building, $E[\text{Loss}_C | \text{IM}]$; ii) the losses due to the repairs, considering that the building has not collapsed, $E[\text{Loss}_{NC \cap R} | \text{IM}]$; and, iii) losses from the demolition of the building due to excessive residual drifts, $E[\text{Loss}_{NC \cap D} | \text{IM}]$. Being $P(C | \text{IM})$, the probability of collapse that the structure will have for a certain IM and $P(D | NC, \text{IM})$, the probability that the structure will have to be demolished if it has not collapsed for a certain IM.

$$E[\text{Loss}_T | \text{IM}] = E[\text{Loss}_C | \text{IM}] \cdot P(C | \text{IM}) + E[\text{Loss}_{NC \cap R} | \text{IM}] \cdot \{1 - P(D | NC, \text{IM})\} + E[\text{Loss}_{NC \cap D} | \text{IM}] \cdot \{P(D | NC, \text{IM}) \cdot \{1 - P(C | \text{IM})\}\}$$

Each DS corresponds to different actions to repair the structural elements damaged: DS1 produces light visible cracking in concrete; DS2 corresponds to wider cracks; DS3 involves the spalling of the concrete cover, the crushing of concrete and the buckling of rebars; DS4 implies the shear failure or the loss of vertical resistance capacity. The repair losses due to the repair of the structure are calculated as the sum of the losses ($E[\text{Loss}_i | \text{IM}]$) of each individual structural and non-structural components of the building, considering the damage states and the probability of being in each of these states. For further information, the procedure established in (Aslani and Miranda, 2005) is to be referred.

The losses expected of structural and non-structural components is normalised by the average replacement cost of the component. In the case of the structural components, their cost has been estimated as a ratio considering the replacement cost of the case study building, the volume of the element and the volume of the structure. The replacement cost of the building has been evaluated by multiplying the total constructed area by an average construction cost per area. This datum has been defined according to the simplified approach for the calculation of Seville's construction cost (Official College of Architects of Seville [Colegio Oficial de Arquitectos de Sevilla], 2021) (Table 1). The damage and the costs of acceleration-and drift-sensitive non-structural components have been calculated following the HAZUS approach as in (Aslani

and Miranda, 2005). Following this, in addition, the losses associated with non-structural components have been computed using a storey-based approach. These represent approximately 20% of the total building replacement cost (Aslani and Miranda, 2005).

3. Numerical modelling

3.1. Description of the case study

A real RC infilled frame case study building located in Seville (Spain) has been considered for the analyses (Fig. 3). The building was constructed in the 70s, before the application of restrictive seismic codes. Therefore, it was only designed considering gravitational loads. Furthermore, it presents a considerable seismic vulnerability due to its soft-storey mechanism located in the ground floor, the irregularities in plan due to the infills distribution, the degradation and the low quality of the materials and the inadequate reinforcement ratios. The building has shallow footings of $1.20 \times 1.20 \times 0.80$ m. The dimension of the RC columns is 30×30 cm. It presents RC wide beams of 30×25 cm and RC ribbed slabs. The reinforcement areas are 8.30 cm^2 and 6.13 cm^2 for the columns and beams, respectively. The infills are composed of 24 cm thick masonry walls. The infills (I) have been shown in (Fig. 3), in the X (X) and Y (Y) directions. They have been named according to the floor (ground floor, 0 and type floor, 1) followed by the number of infills at the storey.

3.2. Superstructure and foundation

The nonlinear behaviour of the RC has been simulated by means of the distributed plasticity approach as in (Couto et al., 2020). To do so, 'nonlinearBeamColumn' elements have been used along the length of the members. The 'RectangularFiberSection' available in STKO has been used to specifically model both the longitudinal and the transverse reinforcement of the RC elements. Uniaxial materials 'Concrete02' and 'Steel02' have been used to model the nonlinear behaviour of the structural materials. The compressive strength and strain of the concrete core have been simulated using the Mander-Priestley model. The 'section aggregator' command and an additional 'modIMKPinching' uniaxial material have been added to the fibre section to account for the real shear behaviour of the section. Second order ($p-\Delta$) effects have been considered by using '3Dforcebeam' to model the RC frames. The mechanical parameters of the structural elements are listed in Table 2. The Rayleigh damping has been considered and it has been assigned to the elements modelled. A 5% damping ratio (ξ) has been considered for the RC superstructure.

Where: concrete compressive (f_c) and crushing strength (f_{cu}); concrete strain at maximum (ϵ_c) and ultimate strength (ϵ_{cu}); steel yielding strength (f_y); steel modulus of elasticity (E_s); infills shear modulus (G_w); post-capping degrading branch coefficient (α); (τ_{cr}); masonry elasticity modulus (E_w).

The infills have been simulated by means of the two-diagonal truss approach using the hysteretic material available in OpenSees (Celarec et al., 2012). They have been connected to the superstructure with 'EqDOF' constraints. The ageing effects have been considered by means of the induced chloride corrosion of the steel and the elimination of the concrete cover depending on the level of exposure of the RC elements. The effects of the rigid RC diaphragms have been borne in mind using the 'rigidDiaph' constraint. Further information on the assumptions concerning the modelling of the structure as well of the ageing effects can be found in (Requena-Garcia-Cruz et al., 2022a; Couto et al., 2020).

3.3. Soil characterisation

The information to characterise the soil has been compiled from a nearby geotechnical study. Four different layers of soil have been determined (Fig. 4): fill, brown clay, brown sand and gravel. According

Table 1
Replacement cost of the case study building.

| Parameter | Value |
|-----------------------|---|
| N° of floors | 5 |
| Dimensions | 18.90×17.30 m, 327 m^2 |
| Total area | 1635 m^2 |
| Cost per m^2 | 627 €/m^2 |
| Replacement cost | 1,025,145 € |

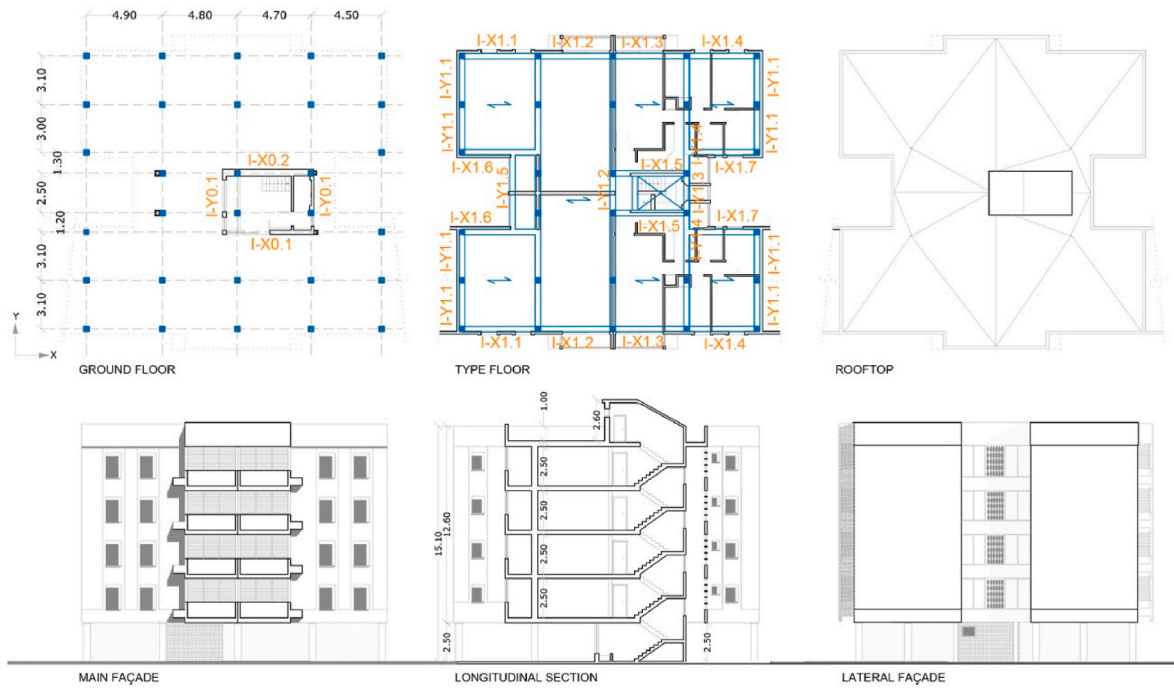


Fig. 3. Schematic configuration of the case study building.

Table 2
Mechanical parameters of the structural elements.

| Concrete | | Steel | | Infills | |
|---------------------|-------|-------------|-----|-------------------|------|
| f_c (MPa) | 28 | f_y (MPa) | 370 | G_w (GPa) | 1240 |
| f_{cu} (MPa) | 4 | E_s (GPa) | 310 | α | 0.05 |
| ϵ_c (%) | 0.002 | | | τ_{cr} (MPa) | 280 |
| ϵ_{cu} (%) | 0.04 | | | E_w (GPa) | 4092 |

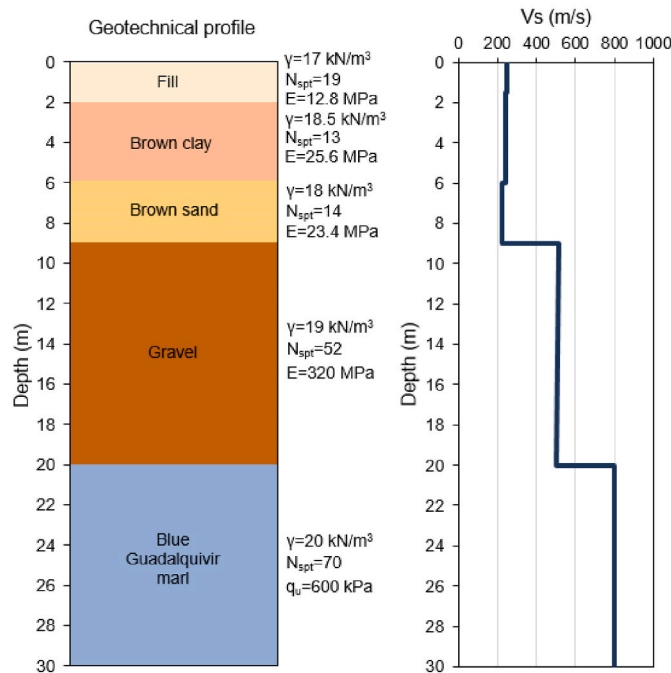


Fig. 4. Geotechnical profile.

to the results of the standard penetration tests (SPT), the first three layers can be classified as low-dense soils ($N_{spt} \approx 11-30$) while the gravel is dense ($N_{spt} \approx 31-50$). The shear wave velocity (V_s) has been computed according to the Imai equation (Naik et al., 2014), which is widely accepted for this type of soil. According to the V_s values and to the soils classification proposed by (Paolucci et al., 2021a), the soil is mainly soft ($V_s < 180$ m/s) and medium-soil (180 m/s $< V_s < 360$ m/s). V_s is also used to define the three parameters needed to define the soil behaviour in the direct modelling of the soil: shear (G), elastic (E) and bulk (B) moduli. The results have been performed under undrained conditions since this is the most restrictive situation for clayey soils. The soil constitutive behaviour has been simulated by means of the ‘Pressur-IndependMultiYield’ (PIMY) material and the ‘upgradestagematerial’ command to behave as nonlinear. The failure criterion of this material is based on the Von Mises’ multi-surface plasticity theory. ‘EqDOF’ has been applied to the interaction between the soil and the foundation surfaces. The volume of the soil is of $108 \times 103 \times 9$ m (X, Y and Z directions). ‘SSPbrick’ brick elements have been applied to the solid elements to capture the soil small deformation. The mesh has 20,776 nodes and 126,729 elements. As suggested by (Paolucci et al., 2021b), the depth of the solid volume has reached the first rigid soil layer with $V_s > 360-800$ m/s. In this case, the gravel.

For the gravitational step and the NLSA, the lateral boundaries have been fixed in the corresponding direction and at the base, in all directions. Nevertheless, for the IDA, the boundaries’ conditions have been varied. The viscous boundary developed by Lysmer and Kuhlemeyer has been used (Lysmer and Kuhlemeyer, 1969). This is based on the use of independent dashpots attached to the boundary in the normal and shear directions. The viscous normal and shear tensions have been computed according to the equations proposed in (Lysmer and Kuhlemeyer, 1969), considering the properties of the soil layer.

4. Analysis of the results

4.1. Modal and nonlinear static analyses

First, a modal analysis of each model has been carried out. In Fig. 5, the results for the FB-model, without considering the SSI effects are

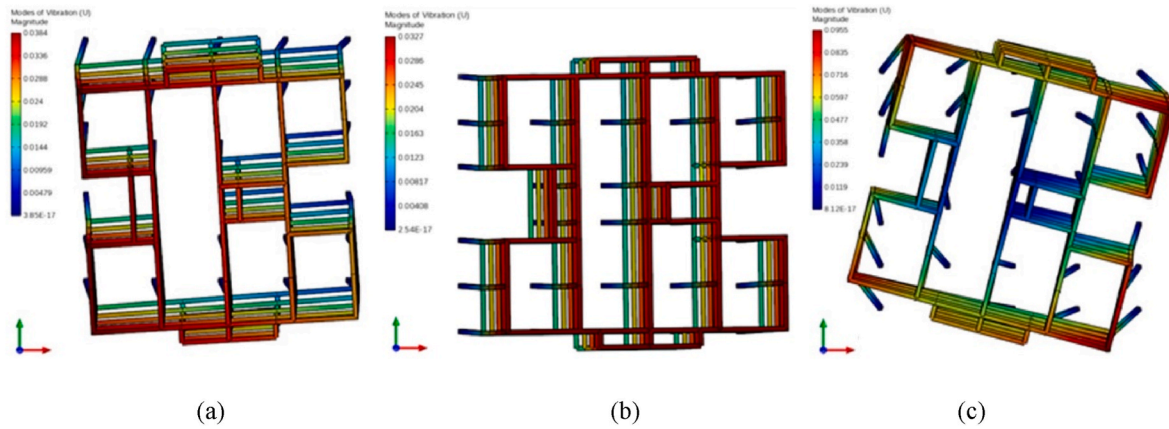


Fig. 5. FB-model modal results (in plan): (a) Mode 1, (b) Mode 2 and (c) Mode 3.

shown. It can be seen that Mode 1 and 2 are translational in the Y (green axis) and X (red axis) directions, respectively. In both cases, more than 75% of the masses are moved. Mode 3 is mainly torsional. Similar results are obtained for the CS-model, which considers the SSI (Fig. 6). The periods for the FB are 0.39 and 0.49 for each mode, respectively. In the case of the CS model, the periods are 0.70 and 0.73 for each mode, respectively. These models cannot be directly compared as, in the second model, the mass of the volume of soil is considered. Nevertheless, it can be useful to prove that the SSI has been properly considered. Moreover, in future analyses, this variation in the values of the periods will lead to different damping ratios as well as a dynamic behaviour.

The results from the NLSA have been plotted in Fig. 7 for the single degree of freedom (SDOF) system (defined according to the N2-method). They have been normalised by dividing the basal shear (V_b) by the total weight (W_{tot}) and the rooftop displacement (d_{top}) by the total height (H_{tot}) of the building. The differences on the seismic behaviour in each direction depend mainly on the irregularities in the plan of the building as in (Requena-Garcia-Cruz et al., 2022c). As can be observed, the position of the staircase is symmetrical in the X axis while not in the Y axis. Hence, this produces a stiffness difference in each direction. Therefore, there is a worse behaviour in the Y direction due to the eccentricity and torsional effects produced. In addition, at the ground floor, there are some infills in the X direction that improve its behaviour. Furthermore, owing to its ‘H-shaped’ plan, the ring beam does not continue along the perimeter, which worsens the stress transfer to the columns in the Y direction. As can be observed in Fig. 7, the effect of the infills is low. For the FB model, the peak strength is improved by the effects of infills, just 19 and 13% in the X and Y directions, respectively, compared to the residual strength of the RC frame structure. For the CS model, the increase is 14 and 10% in the X and Y directions, respectively. Therefore, despite the structure having more infills in the Y direction, they do not produce a significant improvement of its behaviour in this direction.

It can be observed that, in this case, the SSI considerably affects the

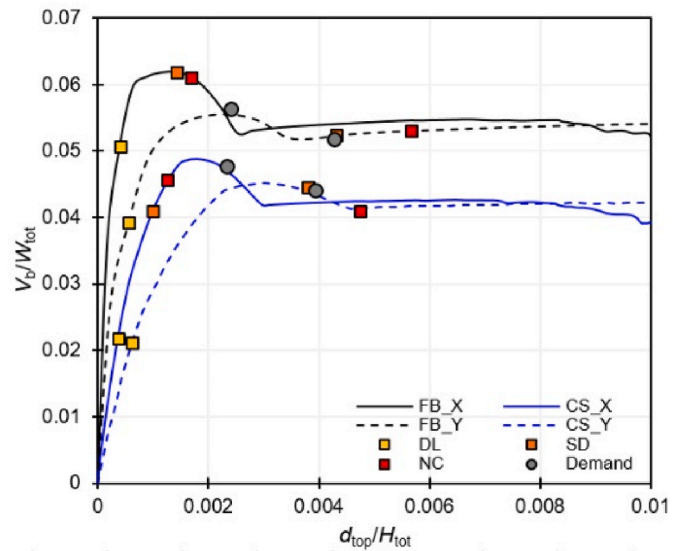


Fig. 7. Normalised SDOF-NLSA curves considering the LS and the demand for each model and direction (X and Y).

capacity and the performance of the building since the peak strength has decreased by up to 12%. In addition, when comparing the damage obtained for the different models, it has been observed that the worse results have also been obtained for the CS-model. In the case of the severe damage state (SD) (which is the state established in the EC8 that residential buildings should comply with), it is obtained that the CDR for the X direction is 0.60 and 0.43 for the FB and CS models, respectively. In the Y direction, it is 1.0 and 0.96. Therefore, the building will not comply with the seismic safety requirements established in the EC8.

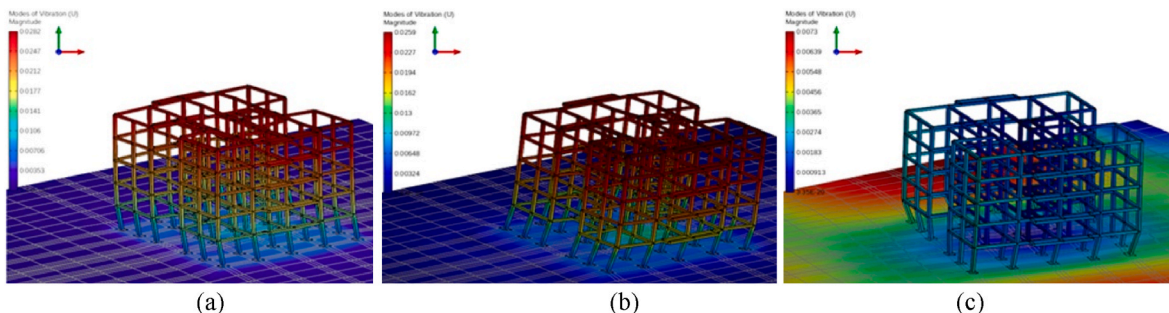


Fig. 6. CS-model modal results (in 3D): (a) Mode 1, (b) Mode 2 and (c) Mode 3.

Furthermore, it can be observed that the damage can worsen by up to 38% if the SSI is considered.

4.2. Incremental dynamic analysis

The results from the IDA are shown in this section. Two types of EDPs have been considered, expressed as the interstorey drift ratio (IDR) and the peak floor acceleration (PFA). Fig. 8 shows the IDA curves for each model, considering each GM and the average values obtained. The IDR has been computed as the average value obtained for the X and Y directions of the structure at the control node. The results depicted in Fig. 8 show that the curves for the CS model present a weaving behaviour (Arshadi, 2016). By contrast, the curves for the FB model show a severe hardening behaviour.

In Figs. 9 and 10, $E[PFA|IM = Sa]$ and the $E[IDR|IM = Sa]$ and represent, respectively, the PFAs and the IDRs expected (mean considering different GMs in the X and Y directions) and for different seismic intensity levels (in total, 5). As can be observed, the values of the expected PFA are higher for the CS model compared to the FBs. These differences are higher for higher levels of IM and for the upper floors. In the case of the IDR assessment, higher ratios can be found at the ground floor, showing that this is the most vulnerable part of the structure. The damage will be concentrated in this part due to its soft-storey mechanism. The IDR values are increased if the SSI is considered. Similar to the results obtained for the PFA, the intermediate floors will not present considerable differences in the IDR. However, at the upper floor this value increases.

The probability of reaching or exceeding each damage state is computed by means of fragility curves. In Fig. 11, the fragility curves for each model are plotted, bearing in mind the demand displacement, computed according to the N2-method. It can be observed that the curves obtained for the CS models are worse than for the FBs. Therefore, the probability of reaching higher values of damage increases. Focusing on the NC LS, for the expected seismic demand, the probability can increase by up to 20% (from 65% to 78%, in the X direction). In the Y direction, the probability can increase by up to a 11%.

In Fig. 12, the variation of the economic losses of each model as a function of the ground motion intensity level is shown. These losses are calculated as the sum of the non-collapse losses due to repairs, the non-collapse losses due to demolitions and the collapse losses. The expected (mean) losses have been expressed, for the different elements, for the near collapse damage state, $E[L_j|NC,IM]$. They have been expressed as a percentage of the replacement cost of the building. As can be observed, the losses expected for the CS-model are considerably higher than those for the FB-model. For the 0.09 g PGA, which is the ground acceleration set for Seville, the losses expected for the FB and the CS-model are 0.07% and 0.17% of the replacement cost of the building, respectively. This represents an outstanding increase of up to 140% of the losses if the SSI

is considered for the case study building. It can be observed that the acceleration-sensitive elements have a negligible expected loss. Structural components represent an important portion of the expected losses. Nonetheless, the main losses stem from the drift-sensitive elements, such as infills.

5. Conclusions

This manuscript aims to investigate if the SSI affects the seismic performance and the losses of RC buildings. To do so, a real 5-storey RC building has been selected as the case study. It was built prior to Spanish seismic codes on soft soil and it has a soft-storey mechanism. The SSI has been modelled by means of the direct method in OpenSees, calibrating both the soil behaviour and the boundary conditions. The direct method has been selected to perform exhaustive analyses (this enables modelling the complete system: structure + foundation + soil) and to provide realistic results compared to methods based on the addition of nonlinear springs.

NLSA have been carried out to assess the capacity and the performance of the models. For the case study, it has been obtained that the peak strength has decreased by up to 12% if the SSI is considered. In order to assess the seismic safety, the capacity/demand ratio has been borne in mind. It has been obtained that the building does not comply with the seismic safety established in the EC8, obtaining values below the requirement of up to 50%. Therefore, it can be concluded that the building must be retrofitted. When comparing the damage expected, it has been obtained that the severe damage can worsen by up to 38% if the SSI is considered.

IDA have been performed to assess the seismic behaviour and the fragility of the case study building. The values of the PFA expected are higher for the CS model compared to the FBs. These differences are bigger for higher levels of IM and for the upper floors. For the IDR assessment, higher ratios can be found at the ground floor. This is due to its soft-storey mechanism, showing that this is the most seismically vulnerable part of the building.

The losses assessment has revealed that higher economic costs are obtained if the SSI is considered as a function of the ground motion intensity. It has been obtained that the economic costs can be increased by up to a 140% by considering the soil effects.

The analyses carried out in this work reveal that when considering the CS-model the building is much more vulnerable than when contemplating the FB-model, since the soil in Seville is characterised by the presence of soft strata over rigid ones at a considerable depth, which amplifies the seismic action. These strata are mainly alluvial soils poorly consolidated, such as fill, clays and silty sands. According to their V_s values and to the soils classification proposed by (Paolucci et al., 2021a), these strata are soft- ($V_s < 180$ m/s) and medium-soils (180 m/s $< V_s < 360$ m/s). Therefore, in the analysis carried out: i) the seismic capacity

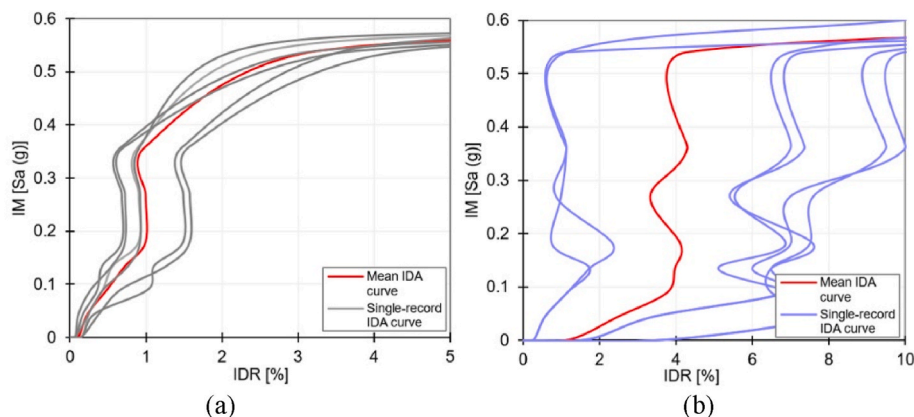


Fig. 8. Single-record and mean IDA curves obtained for the FB (a) and CS (b) models.

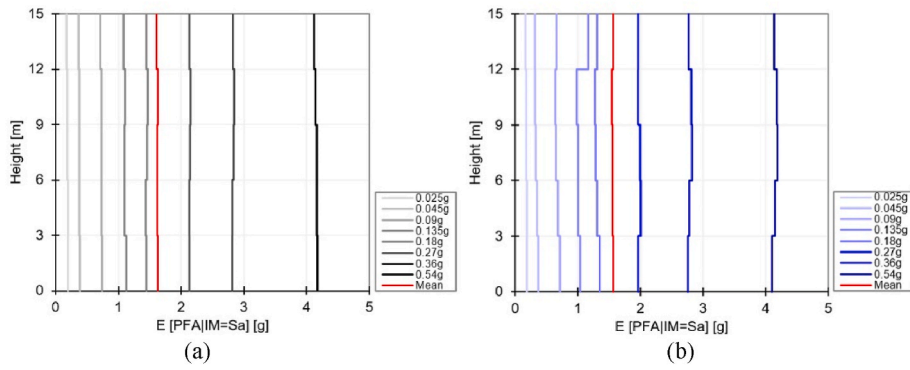


Fig. 9. EDP expressed as PFA and as a function of the building levels for the FB (a) and CS (b) models.

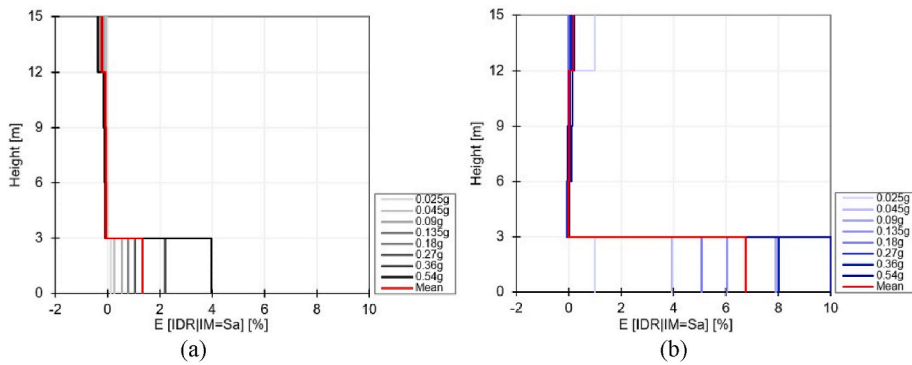


Fig. 10. EDP expressed as IDR and as a function of the building levels for the FB (a) and CS (b) models.

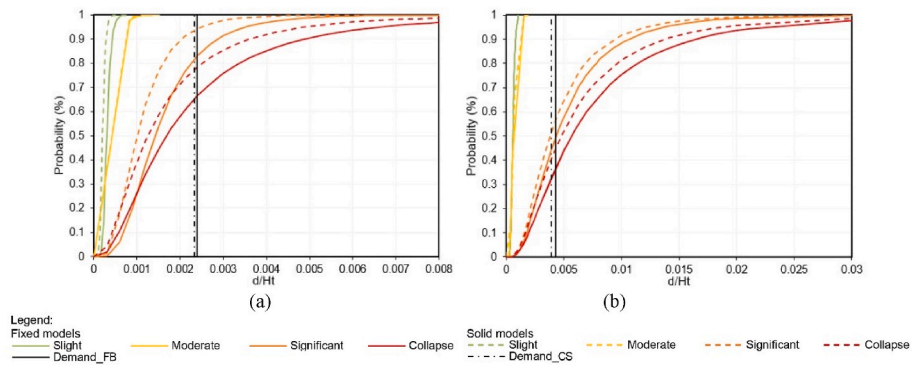


Fig. 11. Fragility curves considering the FB and the CS models, for the X (a) and Y (b) directions.

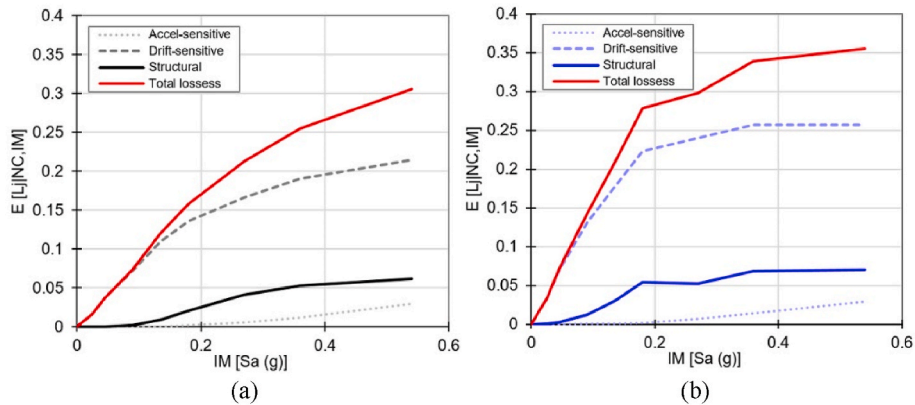


Fig. 12. Loss curves considering the structural elements and non-structural acceleration, and drift-sensitive components for the FB (a) and the CS (b) models.

of the building decreases if the SSI is borne in mind, leading to a worse seismic performance; ii) the fragility curves for the model considering the SSI show a worse seismic damage than the fixed model; and finally, iii) the economic losses are increased if the SSI is taken into account for the same seismic hazard. Hence, it can be concluded that, for this type of building and soil, the consideration of the SSI alters its structural performance and its fragility, which, in this case, have been worsened. This significantly affects the expected economic losses.

Finally, the authors would like to point out the importance of considering the economic losses and not only the seismic safety verification. This should be especially taken into account for decision making and emergency planning. Aspects like the economic losses associated with repair/replacement actions, the disruption in the use of the buildings or the relocation of occupants should be considered to quantify the consequences of an earthquake. Furthermore, these economic indicators can be more easily used by stakeholders and engineers in decision-making management rather than other more complex structural/physical parameters.

Declaration of competing interest

The authors declare that they have no known competing financial interests or personal relationships that could have appeared to influence the work reported in this paper.

Data availability

Data will be made available on request.

Acknowledgements

This work has been supported by the Spanish Ministry of Science and Innovation through the PID2020-117207RB-I00 project and the VII-PPI of the University of Seville by the granting of a scholarship. The funding provided by the *Instituto Universitario de Arquitectura y Ciencias de la Construcción* is also acknowledged.

References

- Anand, V., Satish Kumar, S.R., 2018. Seismic soil-structure interaction: a state-of-the-art review. *Structures* 16, 317–326. <https://doi.org/10.1016/j.istruc.2018.10.009>.
- Arboleda-Monsalve, L.G., Mercado, J.A., Terzic, V., Mackie, K.R., 2020. Soil-structure interaction effects on seismic performance and earthquake-induced losses in tall buildings. *J. Geotech. Geoenviron. Eng.* 146, 04020028 [https://doi.org/10.1061/\(asce\)gt.1943-5606.0002248](https://doi.org/10.1061/(asce)gt.1943-5606.0002248).
- Arshadi, H., 2016. An overview on the concepts and methodologies of incremental dynamic analysis IDA (with a single record and multiple records). In: *World Congress on Structures*.
- Asadi-Ghoozhdi, H., Attarnejad, R., Masoodi, A.R., Majlesi, A., 2022. Seismic assessment of irregular RC frames with tall ground story incorporating nonlinear soil-structure interaction. *Structures* 41, 159–172. <https://doi.org/10.1016/j.istruc.2022.05.001>.
- Aslani, H., Miranda, E., 2005. *Probabilistic Earthquake Loss Estimation and Loss Disaggregation in Buildings*. Department of Civil and Environmental Engineering, Stanford University, CA, p. 383, 94305-4020.
- Behnamfar, F., Banizadeh, M., 2016. Effects of soil-structure interaction on distribution of seismic vulnerability in RC structures. *Soil Dynam. Earthq. Eng.* 80, 73–86. <https://doi.org/10.1016/j.soildyn.2015.10.007>.
- Bommer, J., Spence, R., Erdik, M., Tabuchi, S., Aydinoglu, N., Booth, E., Del Re, D., Peterken, O., 2002. Development of an earthquake loss model for Turkish catastrophe insurance. *J. Seismol.* 6, 431–446. <https://doi.org/10.1023/A:1020095711419>.
- Cardone, D., Perrone, G., 2015. Developing fragility curves and loss functions for masonry infill walls. *earthquake Struct.* 9, 257–279. <https://doi.org/10.12989/eas.2015.9.1.257>.
- Cardone, D., Perrone, G., 2017. Damage and loss assessment of pre-70 RC frame buildings with FEMA P-58. *J. Earthq. Eng.* 21, 23–61. <https://doi.org/10.1080/13632469.2016.1149893>.
- Caruso, C., 2019. *Seismic Retrofit Options for an Old RC Wall-Frame Building in Lisbon: Impact on Loss Estimation and Cost-Benefit Analysis*. Instituto Técnico Superior, Universidade de Lisboa, Portugal.
- Caruso, C., Bento, R., Castro, J.M., 2019. A contribution to the seismic performance and loss assessment of old RC wall-frame buildings. *Eng. Struct.* 197 <https://doi.org/10.1016/j.engstruct.2019.109369>.

- Celarec, D., Ricci, P., Dolšek, M., 2012. The sensitivity of seismic response parameters to the uncertain modelling variables of masonry-infilled reinforced concrete frames. *Eng. Struct.* 35, 165–177. <https://doi.org/10.1016/j.engstruct.2011.11.007>.
- Couto, R., Requena-García-Cruz, M.V., Bento, R., Morales-Esteban, A., 2020. Seismic capacity and vulnerability assessment considering ageing effects. Case study: three local Portuguese RC buildings. *Bull. Earthq. Eng.* 1–24. <https://doi.org/10.1007/s10518-020-00955-4>.
- European Union, Eurocode-8, 2005. *Design of Structures for Earthquake Resistance. Part 3: Assessment and Retrofitting of Buildings*. Brussels, Belgium. <http://www.phd.eng.br/wp-content/uploads/2014/07/en.1998.3.2005.pdf>.
- Fajfar, P., Gašpersič, P., 1996. The N2 method for the seismic damage analysis of RC buildings. *Earthq. Eng. Struct. Dynam.* 25, 31–46 [https://doi.org/10.1002/\(SICI\)1096-9845\(199601\)25:1<31::AID-EQE534>3.0.CO;2-V](https://doi.org/10.1002/(SICI)1096-9845(199601)25:1<31::AID-EQE534>3.0.CO;2-V).
- Kamal, M., Inel, M., Cayci, B.T., 2022. Seismic behavior of mid-rise reinforced concrete adjacent buildings considering soil-structure interaction. *J. Build. Eng.* 51, 104296 <https://doi.org/10.1016/j.jobbe.2022.104296>.
- Khosravikia, F., Mahsuli, M., Ali Ghannad, M., 2018. The effect of soil-structure interaction on the seismic risk to buildings. *Bull. Earthq. Eng.* 16, 3653–3673. <https://doi.org/10.1007/s10518-018>.
- Lysmer, J., Kuhlemeyer, R.L., 1969. Finite dynamic model for infinite media. *J. Eng. Mech. Div.* 95, 859–878.
- McKenna, F., Fenves, G.L., Scott, M.H., 2000. *OpenSees: Open System for Earthquake Engineering Simulation*. Pacific Earthquake Engineering Research Center.
- Mitropoulou, C.C., Kostopanagiotis, C., Kopanos, M., Ioakim, D., Lagaros, N.D., 2016. Influence of soil-structure interaction on fragility assessment of building structures. *Structures* 6, 85–98. <https://doi.org/10.1016/j.istruc.2016.02.005>.
- Morales-Esteban, A., de Justo, J.L., Martínez-Álvarez, F., Azañón, J.M., 2012. Probabilistic method to select calculation accelerograms based on uniform seismic hazard acceleration response spectra. *Soil Dynam. Earthq. Eng.* 43 <https://doi.org/10.1016/j.soildyn.2012.07.003>.
- Naik, S.P., Patra, N.R., Malik, J.N., 2014. Spatial distribution of shear wave velocity for late quaternary alluvial soil of Kanpur city, northern India. *Geotech. Geol. Eng.* 32, 131–149. <https://doi.org/10.1007/s10706-013-9698-3>.
- National Institute of Building Sciences and Federal Emergency Management Agency (NIBS and FEMA), 2003. *Multi-hazard Loss Estimation Methodology, Earthquake Model, HAZUS MH Technical Manual*. Federal Emergency Management Agency, Washington, D. C.
- Nguyen, H.D., Shin, M., 2021. Effects of soil-structure interaction on seismic performance of a low-rise R/C moment frame considering material uncertainties. *J. Build. Eng.* 44, 102713 <https://doi.org/10.1016/j.jobbe.2021.102713>.
- Official College of Architects of Seville [Colegio Oficial de Arquitectos de Sevilla], 2021. *Simplified method for the computation of construction costs of different type of buildings[Método para el cálculo simplificado de los presupuestos estimativos de ejecución material de los distintos tipos de obras]*. Seville (Spain).
- Paolucci, R., Aimar, M., Ciancimino, A., Dotti, M., Foti, S., Lanzano, G., Mattevi, P., Pacor, F., Vanini, M., 2021a. Checking the site categorization criteria and amplification factors of the 2021 draft of Eurocode 8 Part 1–1. *Bull. Earthq. Eng.* 19, 4199–4234. <https://doi.org/10.1007/s10518-021-01118-9>.
- Paolucci, R., Aimar, M., Ciancimino, A., Dotti, M., Foti, S., Lanzano, G., Mattevi, P., Pacor, F., Vanini, M., 2021b. Checking the site categorization criteria and amplification factors of the 2021 draft of Eurocode 8 Part 1–1. *Bull. Earthq. Eng.* 19, 4199–4234. <https://doi.org/10.1007/s10518-021-01118-9>.
- Petracca, M., Candeloro, F., Camata, G., 2017. *STKO User Manual*. ASDEA Software Technology, Pescara, Italy.
- Pinto, P.E., Franchin, P., 2014. Existing buildings: the new Italian provisions for probabilistic seismic assessment. In: *Geotechnical, Geological and Earthquake Engineering*. Springer, pp. 97–130. <https://doi.org/10.1007/978-3-319-07118-3>.
- Rajeev, P., Tesfamariam, S., 2012. Seismic fragilities of non-ductile reinforced concrete frames with consideration of soil structure interaction. *Soil Dynam. Earthq. Eng.* 40, 78–86. <https://doi.org/10.1016/j.soildyn.2012.04.008>.
- Requena-García-Cruz, M.V., Morales-Esteban, A., Durand-Neyra, P., 2021. Optimal ductility enhancement of RC framed buildings considering different non-invasive retrofitting techniques. *Eng. Struct.* 242, 112572 <https://doi.org/10.1016/j.engstruct.2021.112572>.
- Requena-García-Cruz, M.V., Bento, R., Durand-Neyra, P., Morales-Esteban, A., 2022a. Analysis of the soil structure-interaction effects on the seismic vulnerability of mid-rise RC buildings in Lisbon. *Structures* 38, 599–617. <https://doi.org/10.1016/j.istruc.2022.02.024>.
- Requena-García-Cruz, M.V., Morales-Esteban, A., Durand-Neyra, P., 2022b. Assessment of specific structural and ground-improvement seismic retrofitting techniques for a case study RC building by means of a multi-criteria evaluation. *Structures* 38, 265–278. <https://doi.org/10.1016/j.istruc.2022.02.015>.
- Requena-García-Cruz, M.V., Couto, R., Bento, R., Morales-Esteban, A., 2022c. Seismic Assessment of RC Buildings Considering the Influence of Vertical Irregularities: Framed and Wall-Frame Structures, pp. 287–297. https://doi.org/10.1007/978-3-030-83221-6_24.
- Spanish Ministry of Public Works [Ministerio de Fomento de España], 2002. *Spanish Seismic Construction Code of Buildings [Norma de Construcción Sismorresistente: Parte general y edificación (NSCE-02)]*. Spain.

Spanish Ministry of Public Works [Ministerio de Fomento de España], 2012. Update of the seismic hazard maps [Actualización de mapas de peligrosidad sísmica de España]. Spain, Spain.

The MathWorks Inc., MATLAB and Statistics Toolbox Release 2018b, 2018. https://www.researchgate.net/post/How_to_cite_a_Matlab_toolbox_in_academic_research. (Accessed 21 November 2019).

Tomeo, R., Bilotta, A., Pitilakis, D., Nigro, E., 2017. Soil-structure interaction effects on the seismic performances of reinforced concrete moment resisting frames. *Procedia Eng.* 199, 230–235. <https://doi.org/10.1016/J.PROENG.2017.09.006>.